

# All-Electron Path Integral Monte Carlo Simulations of Warm Dense Matter: Application to Water and Carbon Plasmas

K. P. Driver<sup>1,\*</sup> and B. Militzer<sup>1,2</sup>

<sup>1</sup>*Department of Earth and Planetary Science, University of California, Berkeley, California 94720, USA*

<sup>2</sup>*Department of Astronomy, University of California, Berkeley, California 94720, USA*

(Dated: May 25, 2018)

We develop an all-electron path integral Monte Carlo (PIMC) method with free-particle nodes for warm dense matter and apply it to water and carbon plasmas. We thereby extend PIMC studies beyond hydrogen and helium to elements with core electrons. PIMC pressures, internal energies, and pair-correlation functions compare well with density functional theory molecular dynamics (DFT-MD) at temperatures of  $(2.5\text{--}7.5)\times 10^5$  K and both methods together form a coherent equation of state (EOS) over a density-temperature range of  $3\text{--}12$  g/cm<sup>3</sup> and  $10^4\text{--}10^9$  K.

PACS numbers: 62.50.-p, 31.15.A-, 61.20.Ja, 64.30.-t

The development of first-principles methodology for warm, dense matter (WDM) is one of the great challenges of modern materials theory. A need for rigorous simulation of WDM has escalated with intensified interest in advanced energy technologies [1], physics and chemistry of solar and extrasolar planets [2], shock compressed matter [3], and different types of plasma-matter interactions [4]. The standard first-principles method, Kohn-Sham density functional theory molecular dynamics [5] (DFT-MD), produces accurate equations of state in the lower temperature range of the WDM regime. The maximum accessible temperature is limited, however, because the number of partially occupied orbitals eventually becomes computationally intractable [6]. On the other hand, the many-body path integral Monte Carlo (PIMC) method [7] is naturally formulated to study high temperature dependence of materials. Ideally, PIMC and DFT together can produce a coherent equation of state for the entire WDM regime and cross-validate each other at commonly accessible temperatures. However, PIMC has not yet been developed to study systems with core electrons. Indeed, PIMC studies up to now have been limited to plasma states of hydrogen [8–10] and helium [11, 12]. In this letter, we develop an all-electron PIMC method for first-row elements and combine results with DFT-MD to produce comprehensive equations of state for water and carbon in the WDM regime for a density-temperature range of  $3\text{--}12$  g/cm<sup>3</sup> and  $10^4\text{--}10^9$  K.

The central characteristic of a material in the WDM regime is that the electron-ion interaction becomes comparable to the electron kinetic energy and, therefore, effects of bonding, ionization, exchange-correlation, and quantum degeneracy are all important. The analytic methods of condensed matter and plasma physics [13] are typically not reliable without experimental input. One must turn to the numerical, first-principles PIMC and DFT-MD methods which accurately capture the many-body physics in the WDM regime without empirical parameters or corrections. However, first-principles methods utilize certain approximations and one must compare

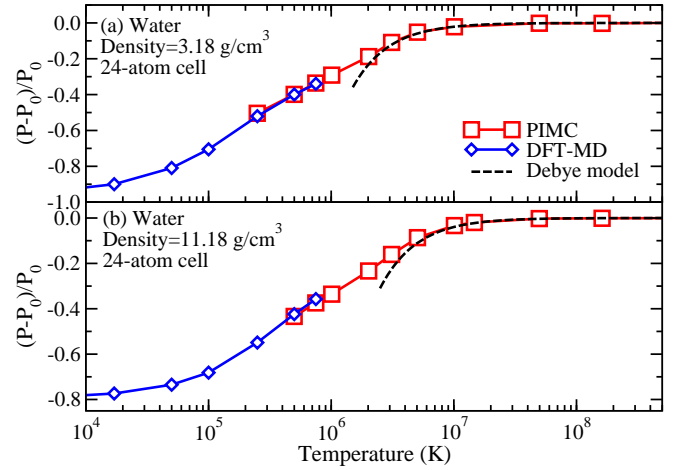


FIG. 1: (color online) Comparison of excess pressure relative to the ideal Fermi gas plotted as a function of temperature for water.

with experimental data if available.

The key approximation in DFT is that of the exchange-correlation potential, which describes all the many body interactions. The exchange-correlation potentials used in nearly all condensed matter calculations are constructed from zero temperature quantum Monte Carlo calculations of the electron gas [14]. In the WDM regime, temperatures are at or above the Fermi temperature and electrons are excited relative to their ground state. Therefore, without further validation, the exchange-correlation potential cannot be assumed to provide an accurate description in the WDM regime.

In DFT calculations it is also common to replace the core electrons in each atom with a pseudopotential. Typically, highest accuracy is obtained with a non-local pseudopotential which depends on the energy and angular momentum components in core states. However, in the WDM regime, it is possible to excite electrons out of core levels. The pseudopotential approximation may break

down and should always be compared with all-electron calculations. Additionally, finite-temperature DFT uses a Fermi-Dirac function to allow for thermal occupation of single-particle electronic states [15], but requires an increasing number of bands with temperature, crippling its efficiency at extreme temperatures. Orbital-free density functional methods aim to overcome such thermal band limitations, but several challenges remain to be solved [16].

The PIMC method avoids the band structure calculation and exchange-correlation approximation by being directly defined from the path integral formulation of quantum statistics. PIMC stochastically solves the full finite-temperature quantum many-body problem by treating electrons and nuclei equally as paths and addresses all of WDM characteristics on an equal footing. All finite-temperature properties of a material are then readily calculated from the thermal density matrix. In contrast to DFT, PIMC efficiency increases with increasing temperature as particles become more classical and fewer time slices are needed, scaling inversely with temperature. A non-local pseudopotential formulation of PIMC does not yet exist [17] and this is why PIMC calculations so far have been limited to hydrogen and helium. PIMC calculations presented here treat all electrons explicitly.

The only uncontrolled approximation in PIMC is that of the nodal surface to deal with the fermion sign problem. Unchecked, the fermion sign problem leads to a cancellation of positive and negative contributions to the density matrix which causes large fluctuations in computed averages. One solution to this problem is the so-called fixed-node approximation in which the location of the nodes are fixed to a known trial nodal structure in order to guarantee positive contributions to the thermal density matrix. The form of the density matrix does not enter the PIMC computation, only the location of the nodes.

The PIMC method we present here employs a free-particle nodal structure, which is expected to be accurate for systems that are almost fully ionized. One could assume accurate calculations of heavier elements requires very high temperatures where atomic cores are ionized also. However, for hydrogen, PIMC with free-particle nodes has provided reliable results at much lower temperatures where only partial ionization occurs [10]. The PIMC results presented for water and carbon here will demonstrate that accurate pressures and energies are obtained for temperatures so low that the 1s states are fully occupied and the 2s states are partially occupied. Analyses of the DFT band occupations show that as the 2s states become less than 60% occupied for  $T \geq 2.5 \times 10^5$  K, PIMC and DFT results agree.

In order to explain this result, we first note that no nodes are needed to describe an isolated, doubly occupied 1s state. Our results for water and carbon indicate that free particle nodes also work in cases where the 1s

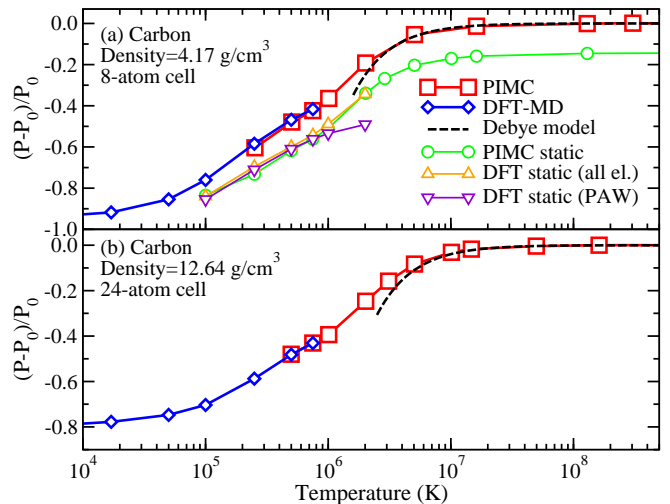


FIG. 2: (color online) Comparison of excess pressures relative to the ideal Fermi gas plotted as a function of temperature for carbon.

state is doubly occupied and all other electrons are ionized. This may be because only one orbital out of many in the Slater determinant is not characterized well. As the occupation of the 2s state exceeds 60% at lower temperatures, the PIMC pressures and energies become inaccurate because free particle nodes cannot yield the correct shell structure around the nucleus [18]. Our results will show, for first-row elements, free particle nodes remain sufficiently accurate at low enough temperatures to overlap with the highest temperature DFT data. This allows the two methods to cross-validate each other and form a single coherent equation of state for all temperatures.

As a first application to test our method, we study water because it is one of the most prevalent materials in nature and knowledge of its electronic properties in the WDM regime is crucial for understanding aspects of astrophysical objects, such as the interiors of giant gas planets. Reports suggest Uranus, Neptune, Jupiter, and Saturn contain significant amounts of water [19–21]. In addition to its rich solid and fluid phases, water is known for its superionic and plasma phases as well as an insulator-to-metal transition at extreme densities and temperatures. Recent DFT-MD simulations [22] have computed the equation of state of water up to  $2 \times 10^4$  K and  $15 \text{ g/cm}^3$ , improving upon the older SESAME 7150 [23] table comprised of a number of analytic models and MD using empirical potentials.

As a second application, we study carbon at high pressures and temperatures for its importance in future energy technologies. In inertial confined fusion experiments, carbon is used as an ablator for target capsules. The performance of the ablator is heavily dependent on the equation of state in the WDM regime [24]. There have been a number of attempts to construct carbon

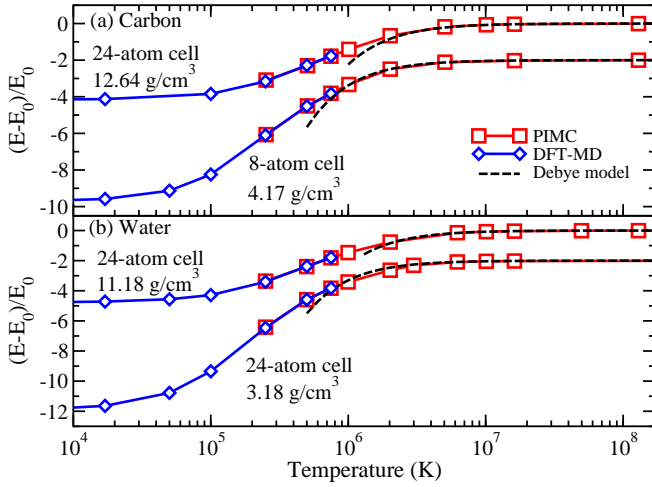


FIG. 3: (color online) Comparison of excess internal energies relative to the ideal Fermi gas plotted as a function of temperature for (a) carbon and (b) water. The lower density data has been shifted by a constant, -2, in both cases.

equations of state in the WDM regime, including free energy models [25, 26] and DFT-MD [27], but they ultimately resort to more approximate Thomas-Fermi-based models that cannot describe any chemical bond.

For our PIMC simulations, the Coulomb interaction is incorporated via pair density matrices derived from the eigenstates of the two-body Coulomb problem. A sufficiently small time step is determined by converging total energy as a function of time step until the energy changes less than 0.2%. For both water and carbon, we use a time step of  $0.0078125 \text{ Ha}^{-1}$  for temperatures below  $5 \times 10^6 \text{ K}$  and, for higher temperatures, the time step decreases as  $1/T$  while keeping at least four time slices in the path integral. In order to minimize finite size errors, the total energy is converged to better than 0.2% for a 24 atom simple cubic cell.

The DFT-MD simulations were performed with either the ABINIT code [28] using all-electron pseudopotentials or with the Vienna *ab initio* simulation package (VASP) [29] using the projector augmented-wave method [30]. MD uses a NVT ensemble regulated with a Nosé-Hoover thermostat. Exchange-correlation effects are described using the Perdew-Burke-Ernzerhof generalized gradient approximation [31]. Electronic wave functions are expanded in a plane-wave basis with a energy cutoff of at least 1500 eV for water and at least 900 eV for carbon in order to converge total energy to chemical accuracy. Size convergence tests indicate that total energies are converged to better than 0.2% in a 24 atom simple cubic cell. Convergence of the number of orbitals to a prescribed thermal occupation of less than  $1 \times 10^{-4}$  requires up to 1500 bands at  $7.5 \times 10^5 \text{ K}$  for a 24-atom cell. All simulations are performed at the gamma-point

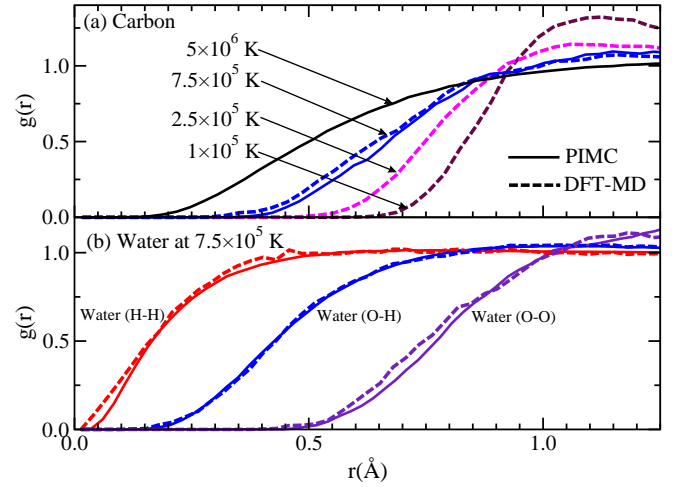


FIG. 4: (color online) Nuclear pair-correlation functions for (a) carbon and (b) water.

of the Brillouin zone, which converges total energy to better than 0.1% at relevant high temperatures.

Figures 1 and 2 compare pressures obtained for water and carbon, respectively, from PIMC, DFT-MD, and Debye-Hückel [32] simulations. Water is studied at fixed densities of 3.18 and 11.18 g/cm<sup>3</sup> and carbon is studied at 4.17 g/cm<sup>3</sup> and 12.64 g/cm<sup>3</sup>. The two densities in each case correspond to a pressure of 1 Mbar and 50 Mbar at zero temperature. Pressures,  $P$ , are plotted relative to a fully ionized Fermi gas of electrons and ions with pressure,  $P_0$ , in order to compare only the pressure contributions that result only from particle interactions. PIMC and DFT-MD results for  $(P - P_0)/P_0$  agree to better than 0.03 in the range of  $2.5 \times 10^5$  to  $7.5 \times 10^5 \text{ K}$ . Convergence tests show that results are equally well converge in 24-atom and 8-atom simulation cells. The excellent agreement allows for cross-validation which implies the zero temperature DFT exchange-correlation potential remains valid at high temperatures and that the free-particle nodal approximation is valid in PIMC when atoms are only partially ionized. The two methods have comparable computational cost in the overlap region, but DFT computational cost starts to become prohibitive beyond  $7.5 \times 10^5 \text{ K}$ , and free particle nodes break down below  $2.5 \times 10^5 \text{ K}$ .

In addition, Fig. 2 compares the instantaneous pressures obtained for a fixed configuration of carbon nuclei at various electronic temperatures using PIMC, DFT with all electron pseudopotentials, and DFT with VASP PAW pseudopotentials. Agreement between PIMC and DFT with all electron pseudopotentials is very good from  $1 \times 10^5$  to  $2 \times 10^6 \text{ K}$ . However, beyond  $7.5 \times 10^5 \text{ K}$ , PAW DFT no longer predicts the correct temperature dependence, indicating that the missing contributions of core excitations to the total energy become significant. All

electron DFT is too computationally demanding to perform calculations with moving nuclei.

In Fig. 3, the internal energies,  $E$ , are plotted relative to the ideal internal energy,  $E_0$ . PIMC and DFT-MD results for  $(E - E_0)/E_0$  agree to better than 0.04 in the range of  $2.5\text{--}7.5 \times 10^5$  K for water and carbon. Convergence tests show that results are equally well converged in 24-atom and 8-atom simulation cells. PIMC extends the equations of state to the weakly interacting plasma limit at high temperatures, in agreement with the Debye-Hückel model. The DFT-MD and PIMC methods together form a coherent equation of state over all temperatures.

Figure 4 shows nuclear pair-correlation functions for carbon and water using PIMC and DFT-MD. Fig. 4(a) demonstrates the sensitive temperature dependence of structural properties for carbon. Water pair-correlations are shown in Fig. 4(b) at a single temperature of  $7.5 \times 10^5$  K. Simulations use a 24-atom simulation cell size, which converges pair-correlation curves to better than 10%. The PIMC and DFT pair correlation curves essentially lie on top of each other with the maximum deviation being 17% for carbon at  $r=0.63$  Å. The results demonstrate that PIMC and DFT predict consistent structural properties in addition to the equation of state.

In conclusion, we have developed an all-electron path integral Monte Carlo method using free-particle nodes that allows for calculations of materials composed of first-row elements and mixtures thereof. Our computations of pressures, internal energies, and pair-correlation functions for water and carbon demonstrate that PIMC and DFT can cross-validate each other in a commonly accessible temperature range and provide an accurate, coherent equation of state ranging from ambient conditions to the plasma limit. The excellent agreement between our PIMC method and DFT-MD validates the use of free-particle nodes for partially-ionized first-row elements and the use of zero-temperature exchange correlation functionals at high temperature.

This research is supported in part by the UC Berkeley lab fee grant and by the NSF. Computational resources were provided by TAC, NCAR, and NERSC.

---

\* Electronic address: kdriver@berkeley.edu;  
URL: <http://militzer.berkeley.edu/~driver/>

[1] I. Cook, Nat. Mater. **5**, 77 (2006).

[2] J. J. Fortney, S. H. Glenzer, M. Koenig, B. Militzer,

D. Saumon, and D. Valencia, Phys. Plasmas **16**, 041003 (2009).

[3] M. Koenig *et al.*, Plasma Phys. Contr. F. **47** (2005).

[4] R. P. Drake, *High-Energy-Density Physics: Fundamentals, Inertial Fusion, and Experimental Astrophysics* (Springer, Berlin, 2006).

[5] J. S. Tse, Annu. Rev. Phys. Chem. **53**, 249 (2002).

[6] M. Surh, I. T. W. Barbee, and L. H. Yang, Phys. Rev. Lett. **86**, 5958 (2001).

[7] D. M. Ceperley, Rev. Mod. Phys. **67**, 279 (1995).

[8] C. Pierleoni, D. M. Ceperley, B. Bernu, and W. R. Magro, Phys. Rev. Lett. **73**, 2145 (1994).

[9] B. Militzer and D. M. Ceperley, Phys. Rev. Lett. **85**, 1890 (2000).

[10] B. Militzer and D. M. Ceperley, Phys. Rev. E **63**, 066404 (2001).

[11] B. Militzer, Phys. Rev. Lett. **97**, 175501 (2006).

[12] B. Militzer, Phys. Rev. B **79**, 155105 (2009).

[13] W. Ebeling and W. D. Kraeft and D. Kemp, *Theory of Bound States and Ionization Equilibrium in Plasmas and Solids* (Akademie-Verlag, Berlin, 1976).

[14] D. M. Ceperley and B. J. Alder, Phys. Rev. Lett. **45**, 566 (1980).

[15] D. N. Mermin, Phys. Rev. **137**, A1441 (1965).

[16] F. Lambert and J. Cléroutin and S. Mazevet, Europhys. Lett. **75**, 681 (2006).

[17] G. E. Jabbour and P. A. Deymier, Modelling Simul. Mater. Sci. Eng. **2**, 1111 (1994).

[18] J. Shumway, in *Computer Simulations Studies in Condensed Matter Physics XVII*, edited by D. P. Landau and S. P. Lewis and H. B. Schütter (Springer Verlag, Heidelberg, Berlin, 2006), pp. 181–195.

[19] N. Nettelmann and B. Holst and A. Kietzmann and M. French and R. Redmer, Astrophys. J. **683**, 1217 (2008).

[20] R. Redmer and T. R. Mattsson and N. Nettelmann and M. French, Icarus **211**, 798 (2011).

[21] P. M. Celliers *et al.*, Phys. Plasmas **11** (2004).

[22] M. French, T. R. Mattsson, N. Nettelmann, and R. Redmer, Phys. Rev. B **79**, 054107 (2009).

[23] S. P. Lyon and J. D. Johnson (1992), Los Alamos Report No. LA-UR-92-3407.

[24] B. A. Hammel *et al.*, Plasma Phys. Contr. F. **48** (2006).

[25] G. I. Kerley and L. Chhabildas (2001), Sandia National Laboratories Report No. SAND2001-2619.

[26] A. Y. Potekhin, G. Massacrier, and G. Chabrier, Phys. Rev. E **72**, 046402 (2005).

[27] A. A. Correa, L. X. Benedict, D. A. Young, E. Schwegler, and S. A. Bonev, Phys. Rev. B **78**, 024101 (2008).

[28] X. Gonze and C. Lee, Comp. Mater. Sci. **25**, 478 (2002).

[29] G. Kresse and J. Furthmüller, Phys. Rev. B **54**, 11169 (1996).

[30] P. E. Blöchl, Phys. Rev. B **50**, 17953 (1994).

[31] J. P. Perdew, K. Burke, and M. Ernzerhof, Phys. Rev. Lett. **77**, 3865 (1996).

[32] P. Debye and E. Huckel, Phys. Z. **24**, 185 (1923).